磁场诱导下 Fe_3S_4 向 FeS_2 转化速率的增加

唐 艳 陈乾旺* 熊 鹰 李 岩
(中国科学技术大学合肥微尺度物质科学国家实验室和材料科学与工程系,合肥 230026)

摘要:以 $FeCl_3$ 和 CH_4N_2S 为主要原料,在 0.2~0.4 T 的外加磁场强度下,温度为 170 ℃的反应体系中研究了磁场对前驱物 Fe_3S_4 转化成 FeS_2 过程的影响。结果表明,Fe_3S_4 到 FeS_2 的转化率是与磁场强度有关的。Fe_3S_4 的硫化过程可能是通过溶解-再结晶机理。外加磁场的存在可以促进物质的传输过程,从而加速前驱物的溶解和再结晶过程,导致和没有外加磁场相比 Fe_3S_4 到 FeS_2 的转化率的增加。

关键词:Fe_3S_4; FeS_2; 磁场; 转化速率
中图分类号:O613.51; O614.81+1 **文献标识码**:A **文章编号**:1001-4861(2007)06-0941-07

Magnetic Field-induced Increase in Conversion Rate of Fe_3S_4 to FeS_2

TANG Yan CHEN Qian-Wang* XIONG Ying LI Yan
(*Hefei National Laboratory for Physical Sciences at Microscale and Department of Materials Science & Engineering, University of Science and Technology of China, Hefei* 230026)

Abstract: The formation of FeS_2 from a Fe_3S_4 precursor in the external magnetic field strength of 0.2~0.4 T has been experimentally examined. In the reaction system of $FeCl_3$-CH_4N_2S at 170 ℃, the conversion rate of Fe_3S_4 to FeS_2 was found to be magnetic field strength dependent. The sulfidation of Fe_3S_4 may proceed via dissolution and precipitation mechanism, the presence of an external magnetic field could promote the mass transport process and then accelerate the dissolution and crystallization processes, resulting in faster conversion rate of Fe_3S_4 to FeS_2 than that in the absence of an applied magnetic field.

Key words: Fe_3S_4; FeS_2; magnetic field; conversion rate

0 Introduction

Magnetic field effects on chemical, physical and biological systems have been extensively studied[1~3]. With the development of superconducting magnets, an essential influence of an external permanent magnetic field on rate of electrochemical reaction has been observed, most of the effects have been interpreted in terms of a magnetohydrodynamics mechanism where the Lorentz force on ions in solution induces convection of solution, resulting in accelerating the mass transport at the electrode and thus increasing the reaction rate[4,5]. Moreover, experiments have showed that Nd-Fe-B permanent magnets generate strong quantifiable convective effects during electrolysis, similar to those obtained with rotating electrodes or large electromagnets[6]. Rapid developments in superconducting magnets have also facilitated studies of magnetic field effects on the orientation, crystal habit, and number of protein crystals[7~9]. The presence of a

收稿日期:2006-11-20。收修改稿日期:2007-03-30。
国家自然科学基金资助项目(No.20321101,20125103,90206034)。
*通讯联系人。E-mail:cqw@ustc.edu.cn;Tel:0551-3607292
第一作者:唐 艳,女,29 岁,博士研究生;研究方向:磁场诱导下的化学反应。

magnetic field can increase or decrease the number or the growth rate of protein crystals because a magnetic field can promote or damp the convection of the solution.

Although magnetic field effects on aqueous solutions have been one of the more popular areas of research, up to now there are no experimental investigations addressing the effect of an external magnetic field on the transformation of Fe_3S_4 in hydrothermal solutions to FeS_2. Here we report the results of experiments performed with and without an external magnetic field. With the aim of getting more insight in the details of the process, we have varied the intensity of an external magnetic field. It is shown that an external magnetic field accelerates the conversion of Fe_3S_4 to FeS_2.

1 Experimental

Chemical reagents used in the experiment including $FeCl_3 \cdot 6H_2O$, formic acid (HCOOH), thiourea (CH_4N_2S), were all analytical grade and purchased from Shanghai Chemical Reagents Company. Thiourea was used as the sulfur source in the experiments because of its ability to produce H_2S by reacting with water. Moreover, hydrogen sulfide, a common component of hydrothermal solutions[10], was used as a sulfur source, which makes possible application of our results to geological systems.

The starting solution was prepared by dissolving 3.463 5 g $FeCl_3 \cdot 6H_2O$ and 1.164 6 g thiourea in 150 mL N_2-purged water, then 6 mL formic acid was added into the mixed solution. It should be noted that no iron sulfide was precipitated at room temperature. Subsequently, the solutions (pH value <4, the pH value of both the final solution and the starting solution was measured at room temperature with a combination electrode (E201-C-9 model)) were transferred into three Teflon-lined stainless steel autoclaves with 60 mL capacity (one without external magnetic field, and two with 0.2 T and 0.4 T external magnetic fields of permanent rare earth Nd-Fe-B magnets, respectively). All of the autoclaves were sealed and maintained at 170 ℃ in a reaction oven with run duration ranged from 6 h up to 72 h. At the end of the experiment, the autoclaves were cooled to room temperature naturally. The filtered black precipitates were washed with carbon disulfide, distilled water and absolute ethanol in sequence, and then vacuum dried at 40 °C for 4 h.

The dried samples were immediately analyzed both quantitatively and qualitatively by powder X-ray diffraction method (XRD). The samples were recorded at a scanning rate of $0.05° \cdot s^{-1}$ over 20°~70° 2θ using a Philips X′pert X-ray diffractometer with germanium monochromatized Cu $K\alpha$ radiation (λ=0.154 056 nm). Quantitative phase analysis was performed on products using the method recommended by Murowchick and Barnes[11]. The contents of Fe_3S_4 and FeS_2 were determined from a standard curve of I(mc) / {I(mc) + I(gr)} vs composition where I (mc) is the sum of the integrated intensities of the FeS_2 (110), (101) and (211) reflections and I(gr) is the sum of the integrated intensities of the Fe_3S_4 (311), (400) and (440) reflections. The curve was constructed using carefully made mixtures of as-prepared pure Fe_3S_4 and FeS_2. Preferred orientation of as-obtained produces was minimized by careful grinding.

The scanning electron microscope (SEM) images was taken on a Hitachi X-650 microscope, sample preparation for SEM following standard techniques, however, the exposure to air was kept to a minimum time. Samples for SEM were stored under vacuum up to the moment of preparation.

2 Results

The result of I(mc) / {I(mc) + I(gr)} vs composition is presented in Fig.1.

The XRD patterns of the products obtained in the presence of a zero, 0.2 T, and 0.4 T external magnetic field are shown in Fig.2, Fig.3 and Fig.4, respectively.

Regardless of the existence of an external magnetic field, the first crystalline phase observed after 6 h was pure Fe_3S_4 (JCPDS No.89-1999); the sharp reflection peaks in XRD pattern indicated good crystallinity. With increasing time of reaction, the

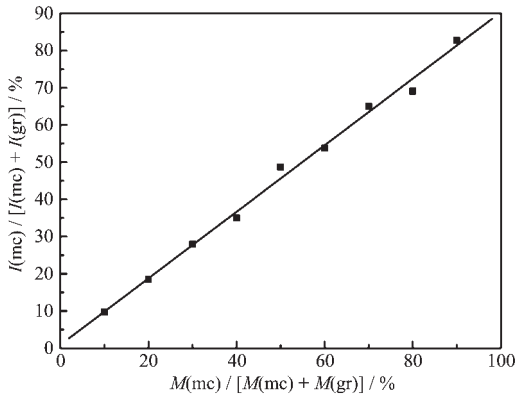

Plot depicts the relationship between the content of FeS_2 in the two-phase mixture and ratio of the summed integrated intensities of the FeS_2 (110), (101) and (211) diffractions to sum of the integrated intensities of the Fe_3S_4 (311), (400) and (440) diffractions and the FeS_2 (110), (101) and (211) diffractions (gr=Fe_3S_4, mc=FeS_2)

Fig.1　A standard curve of I(mc) / [I(mc) + I(gr)] vs composition

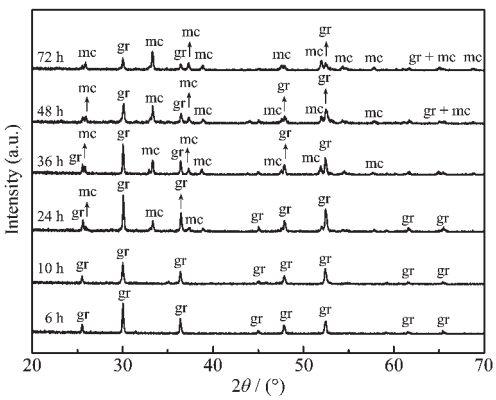

Time range varied from 6 h to 72 h

Fig.2　XRD patterns obtained in the absence of an external magnetic field for $FeCl_3$-CH_4N_2S experiments (gr=Fe_3S_4, mc=FeS_2)

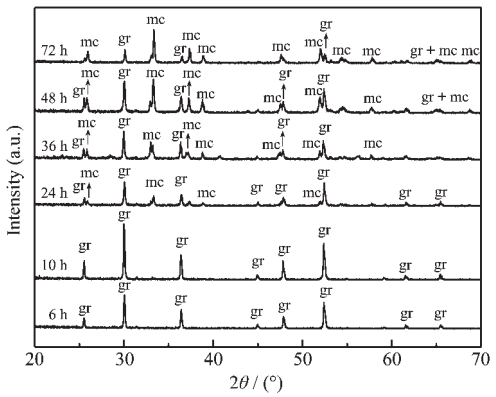

Time range varied from 6 h to 72 h

Fig.3　XRD patterns of reaction products showing the progress of phase evolution in the presence of a 0.2 T external magnetic field for $FeCl_3$-CH_4N_2S experiments (gr=Fe_3S_4, mc=FeS_2)

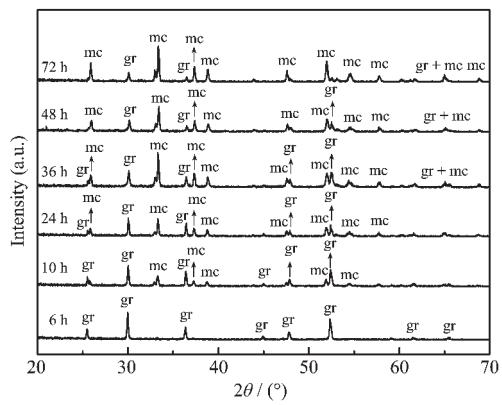

Time range varied from 6 h to 72 h

Fig.4　Stack of XRD patterns showing the conversion progress of Fe_3S_4 to FeS_2 during the sulfidation of Fe_3S_4 in the presence of a 0.4 T external magnetic field for $FeCl_3$-CH_4N_2S experiments (gr=Fe_3S_4, mc=FeS_2)

products consisted of magnetic and nonmagnetic components, indicating the conversion of Fe_3S_4 to FeS_2 (JCPDS No. 88-2282) occurred. The presence of FeS_2 was not detected in the product formed in the presence of a zero, 0.2 T external magnetic field after 10 h, while the product consisted of 34.5% FeS_2 and 65.5% Fe_3S_4 was found for a 0.4 T external magnetic field experiment. 4.6%, 9.9%, 15.7%, 25.1%, 36.0%, 46.6%, and 64.9% of FeS_2 was formed by the precursor Fe_3S_4 in the absence of an external magnetic field for 12, 16, 20, 24, 36, 48, and 72 h, respectively. By contrast, the results of experiments conducted in the presence of an external magnetic field indicated that the transformation of Fe_3S_4 to FeS_2 occurred at a comparable or much faster rate than that of the experiments conducted in the absence of an external magnetic field. In the experiments conducted in the presence of a 0.2 T external magnetic field, 8.5%, 12.6%, 21.0%, 29.0%, 40.6%, 52.3%, 73.5% FeS_2 observed within 12, 16, 20, 24, 36, 48, and 72 h while in the 0.4 T external magnetic field experiments 36.3%, 41.3%, 46.7%, 51.6%, 63.5%, 70.1%, 92.7% of the initial precursor Fe_3S_4 was transformed to FeS_2. Product of Fe_3S_4 to dominantly FeS_2 occurred after 72, 48, 24 h in the presence of a zero, 0.2 T, 0.4 T

external magnetic field, respectively. The detailed conditions and the results of quantitative analyses of XRD patterns for $FeCl_3$-CH_4N_2S experiments at temperature of 170 ℃ are shown in Table 1.

Table 1 Summary of experimental conditions and products at 170 ℃ for $FeCl_3$-CH_4N_2S with and without an external magnetic field

Run	Time / h	Products	I(mc) / [I(mc) + I(gr)] / %	FeS_2 / wt.%
0	6	Fe_3S_4	0	0
0	8	Fe_3S_4	0	0
0	10	Fe_3S_4	0	0
0	12	Fe_3S_4, FeS_2	5.0	4.6
0	16	Fe_3S_4, FeS_2	9.7	9.9
0	20	Fe_3S_4, FeS_2	14.8	15.7
0	24	Fe_3S_4, FeS_2	23.2	25.1
0	36	Fe_3S_4, FeS_2	32.9	36.0
0	48	Fe_3S_4, FeS_2	42.3	46.6
0	72	FeS_2, Fe_3S_4	58.6	64.9
0.2 T	6	Fe_3S_4	0	0
0.2 T	8	Fe_3S_4	0	0
0.2 T	10	Fe_3S_4	0	0
0.2 T	12	Fe_3S_4, FeS_2	8.4	8.5
0.2 T	16	Fe_3S_4, FeS_2	12.1	12.6
0.2 T	20	Fe_3S_4, FeS_2	19.6	21.0
0.2 T	24	Fe_3S_4, FeS_2	26.7	29.0
0.2 T	36	Fe_3S_4, FeS_2	37.0	40.6
0.2 T	48	FeS_2, Fe_3S_4	47.4	52.3
0.2 T	72	FeS_2, Fe_3S_4	66.3	73.5
0.4 T	6	Fe_3S_4	0	0
0.4 T	8	Fe_3S_4, FeS_2	17.6	18.8
0.4 T	10	Fe_3S_4, FeS_2	31.6	34.5
0.4 T	12	Fe_3S_4, FeS_2	33.2	36.3
0.4 T	16	Fe_3S_4, FeS_2	37.6	41.3
0.4 T	20	Fe_3S_4, FeS_2	42.4	46.7
0.4 T	24	FeS_2, Fe_3S_4	46.8	51.6
0.4 T	36	FeS_2, Fe_3S_4	57.4	63.5
0.4 T	48	FeS_2, Fe_3S_4	63.3	70.1
0.4 T	72	FeS_2, Fe_3S_4	83.4	92.7

SEM images of products progressively for longer time provide a clue as to how the conversion proceeds (see Fig.5). The morphologies of greigite for 6 h without and with a 0.2 T applied magnetic field (Fig. 5a and 5b) are irregular, fine-grained. However, with a 0.4 T applied magnetic field, the morphologies of greigite are polyhedrical (Fig.5c). Flower-like marcasite morphologies are observed for 24 h without an external magnetic field (Fig.5d). Large scale marcasite aggregates comprised of euhedral crystals are present in the products prepared with a 0.2 T external magnetic field (Fig.5e). Aligned marcasite aggregates are observed after 24 h with a 0.4 T magnetic field (Fig.5f).

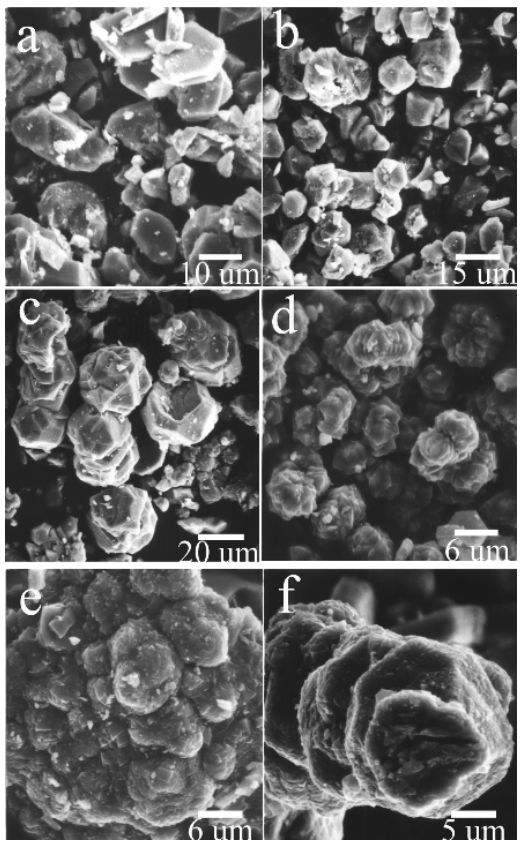

Scale bar is displaced at right lower corner of each photo. (a) Irregular greigite crystals prepared for 6 h without an external magnetic field, (b) Irregular greigite crystals prepared for 6 h in the presence of a 0.2 T magnetic field applied, (c) Polyhedron greigite crystals for 6 h with a 0.4 T magnetic field applied, (d) Flower-like marcasite crystals prepared for 24 h without an external magnetic field, (e) Large marcasite aggregates composed of microcrystals for 24 h with a 0.2 T magnetic field applied, (f) Aligned marcasite aggregates composed of microcrystals for 24 h in the presence of a 0.4 T magnetic field applied

Fig.5 SEM microphotographs illustrating the morphologies of the products prepared under the different conditions

3 Discussion

Based on experimental studies, 'H_2S pathway' for FeS_2 formation in aqueous solutions can be represented by the overall reaction[12~14]:

'FeS' + $H_2S \rightarrow FeS_2 + H_2$ (g)　　(**1**)

where 'FeS' corresponds to one of the iron monosulfides (i.e., $Fe_{1+X}S$, or Fe_3S_4). In the $FeCl_3$-CH_4N_2S experiments, S (0) species was formed during reactions of Fe(Ⅲ) in the solution with H_2S, by the yellow solid obtained in the final product in most of the experiments; the elemental sulfur and hydrogen sulfide then become involved in reactions with Fe_3S_4 to produce FeS_2. So the FeS_2-forming reactions can be written as:

Fe_3S_4 (s) + 2S $\rightarrow$ 3FeS_2 (s)　　(**2**)

Fe_3S_4 (s) + 2$H_2S \rightarrow$ 3FeS_2 + 2H_2 (g)　　(**3**)

In this process, two thirds of the Fe(Ⅲ) in Fe_3S_4 is reduced to Fe(Ⅱ), S(0) and hydrogen sulfide as oxidants are involved in the process.

A kinetic study of the equation **1** in aqueous solution shows that the reaction rate can be described by the equation[12]:

$$dm_{FeS_2}/dt = km_{FeS}\, c_{H_2S(aq)} \quad (4)$$

where dm_{FeS_2}/dt is the rate of FeS_2 formation, m_{FeS} is the concentration of iron monosulfide, $c_{H_2S(aq)}$ is the concentration of H_2S (aq), and k is the rate constant. Whereas S(0) is involved in sulfidation process of Fe_3S_4 for $FeCl_3$-CH_4N_2S experiments, the reaction rate can be described as below:

$$dm_{FeS_2}/dt = km_{Fe_3S_4}\, c_{'S'(aq)} \quad (5)$$

where dm_{FeS_2}/dt is the rate of FeS_2 formation, $m_{Fe_3S_4}$ is the concentration of Fe_3S_4, $c_{'S'(aq)}$ represents the concentration of sulfur sources (including S (0) and hydrogen sulfide) and k is the rate constant.

The extent of conversion (y) is a function of reaction time (t). The plots of y vs t was presented in Fig.6 showing the results of the quantitative analyses of XRD patterns for the product obtained under different treatment conditions at 170 ℃ over periods from 6 h to 72 h. In this case, the actual reaction rate (dy/dt) is derived from the curves of y vs t in Fig.6 by differentiating y with respect to t. Fig.7 shows the time function of the reaction rate for $FeCl_3$-CH_4N_2S experiments with and without an applied magnetic field.

In the first stage of reaction, the conversion of

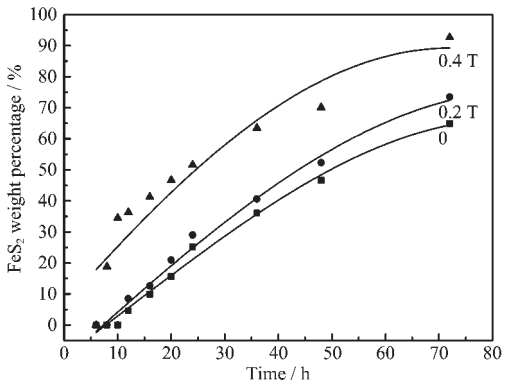

Symbols (▲), (●), and (■) represent the extent of conversion in the presence of a 0.4 T, 0.2 T and 0 external magnetic field, respectively

Fig.6　Extents of reaction (FeS_2 weight percentage) vs time for the products obtained with or without an applied magnetic field

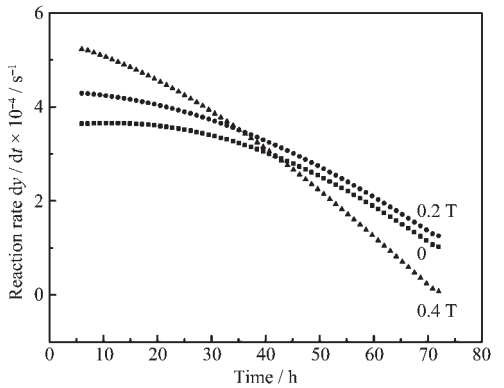

Symbols (▲), (●), and (■) represent the reaction rate in the presence of a 0.4 T, 0.2 T and 0 external magnetic field, respectively

Fig.7　Dependence of reaction rate (dy/dt) on time for $FeCl_3$-CH_4N_2S experiments

Fe_3S_4 to FeS_2 proceeds at a faster rate in the presence of a 0.4 T magnetic field than that with and without a 0.2 T applied magnetic field. As the reaction continues, however, the rates of the conversion of Fe_3S_4 with and without a 0.2 T external magnetic field in Fig.7 are faster than that in the presence of a 0.4 T applied magnetic field. The reason is that more sulfur sources responsible for the formation of FeS_2 are consumed in the presence of a 0.4 T applied magnetic field through the reaction, followed by lower rates of the Fe_3S_4 transformation to FeS_2 than that with and without a 0.2 T applied magnetic field.

Judging from the reaction process comparison between 0, 0.2 T and 0.4 T in the $FeCl_3$-CH_4N_2S

experiments, we conclude that the application of an external magnetic field has a considerable influence on Fe_3S_4 precursor phase transformations, and the presence of an applied magnetic field accelerates chemical transformation process. Based on the SEM morphology of the product in $FeCl_3$-CH_4N_2S experiment with and without an external magnetic field, the mechanism of marcasite formation involves dissolution of precursor iron monosulfide and the subsequent reaction of dissolved iron monosulfide with sulfur sources to yield FeS_2, which is in agreement with the observed kinetics[13~16]. The experiment results indicate that rules of the sulfidation reaction keep unchanged, so does the phase of the products with an applied external magnetic field. Then the reaction process should also be the same to that under zero field, the reaction mechanism can be summarized as below: (a) the dissolution of the precursor Fe_3S_4 crystals; (b) the reaction of aqueous Fe_3S_4 product with dissolved sulfur; (c) the nucleation of FeS_2; and (d) the growth of FeS_2. Together with the temperature dependence of the Arrhenius energy, Rickard and Luther[13] proposed that formation of FeS_2 became more chemically controlled at $T < 50$ ℃ ($E > 40$ kJ·mol^{-1}) and more transport controlled reaction at $T > 50$ ℃ ($E < 40$ kJ·mol^{-1}). The sulfidation process of precursor Fe_3S_4 is transport controlled under our experimental conditions. In the following, we will discuss the mechanism why magnetic field may enhance the mass transport process in more detail.

Different from the field of most commercial electromagnets, the characteristic of the permanent Nd-Fe-B magnet used in our study is the presence of magnetic field gradients, which induces the magnetic force in the solution so that magneto-convection is induced. Hence there are two mass transport processes in the experiments: diffusion and convection. In general, the differential equation for mass transfer in a volume-centered system[17] is

$$\partial c / \partial t = D\nabla^2 c + u\nabla c \quad (\mathbf{6})$$

where c is the solute concentration; D is its diffusion coefficient in solution, assumed not to be a function of concentration; and u is the net effective velocity of flow for transporting solute by convection and a complicated function of c, position, and time t.

Chronoamperometric experiments[6,18] have indicated that the magnetic field does not affect the diffusion coefficients of electroactive species; on the other hand, the magnetic field exerts a clear effect on the conversion rate, which increases with increasing intensity of the magnetic field. Thus $u\nabla c$ is positive according to equation **6**; it is this convection that enhances the diffusion of the precursor Fe_3S_4 crystals and thus the dissolution rate. The results of this experimental study are in accord with the conclusions that magnetic field can enhance convection in a paramagnetic aqueous solution[19,20]. Furthermore, it has been suggested that the magnetic field can increase dissolution of metastable precursor phases and nucleation of more stable phases for calcium phosphate system[21].

The magnitude of the nucleation barrier, ΔG^* depends mainly on the interfacial tension (σ) between a solid and solution, and the affinity of phase change, ϕ[22]:

$$\Delta G^* = \beta\sigma^3 v^2 / \phi^2 \quad (\mathbf{7})$$

where β is a geometrical factor and v is the molecular volume of the solid phase.

The nucleation rate, J increases exponentially with a decrease in the height of the nucleation barrier[22]:

$$J \approx \exp(-\Delta G^*/kT) \quad (\mathbf{8})$$

By studying the magnetic field effect on the *in situ* calcium carbonate precipitation, Hołysz et al.[23] proposed that the magnetic fields decreased surface tension of the sodium carbonate by 1~4 mN·m^{-1} depending on the exposure time. So in the presence of an external magnetic field the decrease of surface tension will lead to the decrease of nucleation barrier ΔG^* for the iron disulfide. The nucleation rate J of the iron disulfide will then increase in the presence of an applied magnetic field. Additionally, the presence of an external magnetic field enhances the delivery of reactive iron and dissolved sulfur to the nucleation site, which encourages FeS_2 nucleation and growth.

The results of this research may be used to understand the possible influence of the Earth′s

magnetic field on transformation rate of iron monosulfide to iron disulfide. FeS_2 is often major constituent of sulfide deposits, whereas Fe_3S_4 as a precursor to FeS_2 has been widely considered to be of importance in most sedimentary sequences despite its metastability with respect to FeS_2. Although magnetic field of the Earth is weak on the surface, the intensity of the mantle′s magnetic field may be comparable to the intensity of permanent rare earth Nd-Fe-B magnets since the strength of magnetic field is inversely related to the square of its distance from the source of the field. In addition, the long time effect of weak geomagnetic field makes it possible that Fe_3S_4 is transformed to FeS_2, providing that there are sufficient intermediate sulfur species to form FeS_2.

4 Conclusions

Experiments have been carried out to investigate whether an external magnetic field has an influence on the transformation rate of Fe_3S_4 to iron disulfide. The conversion proceeds at a faster rate in the presence of an external magnetic field than that without an external magnetic field. The rate of conversion depends on the intensity of a magnetic field applied, which increases with increase in the intensity of an applied magnetic field. It is concluded that an inhomogeneous magnetic field could magnetically induce convection so that the mass transport processes during dissolution of precursor and precipitation of final product are promoted.

References:

[1] Turro N J, Kraeutler B. *Accounts Chem. Res.*, **1980**,**13**:369~377

[2] Steiner U E, Ulrich T. *Chem. Rev.*, **1989**,**89**:51~147

[3] Grissom C B. *Chem. Rev.*, **1995**,**95**:3~24

[4] Ragsdale S R, Grant K M, White H S. *J. Am. Chem. Soc.*, **1998**,**120**:13461~13468

[5] Lioubashevski O, Katz E, Willner I. *J. Phys. Chem. B*, **2004**, **108**:5778~5784

[6] Leventis N, Gao X R. *Anal. Chem.*, **2001**,**73**:3981~3992

[7] Wakayama N I, Ataka M, Abe H. *J. Cryst. Growth*, **1997**,**178**: 653~656

[8] Wakayama N I. *Cryst. Growth Des.*, **2003**,**3**:17~24

[9] Yin D C, Wakayama N I, Inatomi Y, et al. *Adv. Space Res.*, **2003**,**32**:217~223

[10]Barnes H L. *Geochemistry of Hydrothermal Ore Deposits*. New York: J. Wiley & Sons, **1979**.404~454

[11]Murowchick J B, Barnes H L. *Geochim. Cosmochim. Acta*, **1986**,**50**:2615~2629

[12]Rickard D. *Geochim. Cosmochim. Acta*, **1997**,**61**:115~134

[13]Rickard D, Luther G W. *Geochim. Cosmochim. Acta*, **1997**, **61**:135~147

[14]Butler I B, Böttcher M E, Rickard D, et al. *Earth Planet. Sci. Lett.*, **2004**,**228**:495~509

[15]Rickard D T. *Am. J. Sci.*, **1975**,**275**:636~652

[16]Luther G W. *Geochim. Cosmochim. Acta*, **1991**,**55**:2839~2849

[17]Wilcox W R. *Preparation and Properties of Solid State Materials*. New York: Marcel Dekker, Inc., **1976**.129

[18]Hinds G, Spada F E, Coey J M D, et al. *J. Phys. Chem. B*, **2001**,**105**:9487~9502

[19]Nakatsuka K, Hama Y, Takahashi J. *J. Magn. Magn. Mater.*, **1990**,**85**:207~209

[20]Braithwaite D, Beaugnon E, Tournier R. *Nature*, **1991**,**354**: 134~136

[21]Sørensen J S, Madsen H E L. *J. Cryst. Growth*, **2000**,**216**: 399~406

[22]Nielsen A E. *Kinetics of Precipitation*. Oxford: Pergamon Press, **1964**.

[23]Hołysz L, Chibowski M, Chibowski E. *Colloid Surface A*, **2002**,**208**:231~240